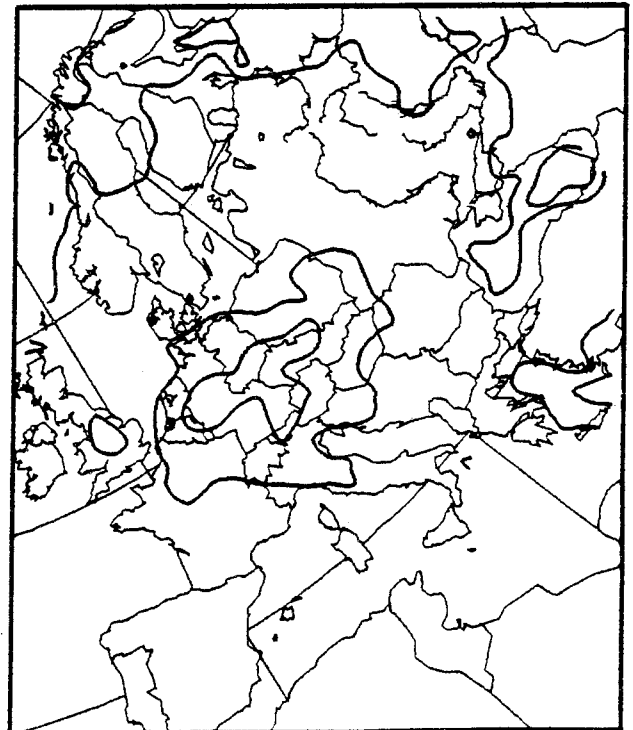
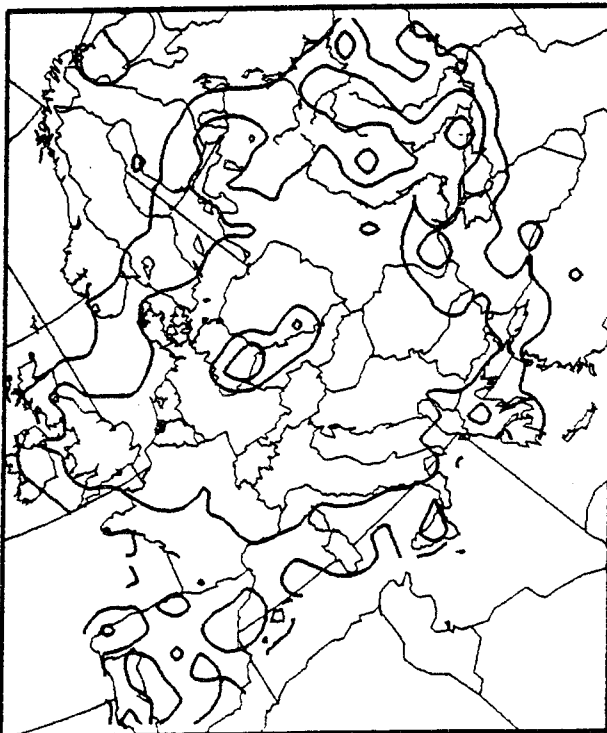


EMEP

CO-OPERATIVE PROGRAMME FOR MONITORING
AND EVALUATION OF THE LONG RANGE
TRANSMISSION OF AIR POLLUTANTS IN EUROPE

Preliminary estimates of sulphur transport and deposition in Europe with a regional scale multilayer Eulerian model.

Erik Berge



MSC-W

METEOROLOGICAL SYNTHESIZING CENTRE - WEST
THE NORWEGIAN METEOROLOGICAL INSTITUTE
P.O. BOX 43-BLINDERN, N-0313 OSLO 3, NORWAY

EMEP/MSC-W Note 1/93.

Date: August 1993.

**Preliminary estimates of sulphur transport and
deposition in Europe with a regional scale multilayer
Eulerian model.**

Erik Berge

Contents

	Page
PREFACE AND ACKNOWLEDGEMENTS	3
1 INTRODUCTION	4
2 METEOROLOGICAL DATA	5
3 DESCRIPTION OF THE EULERIAN AIR POLLUTION MODEL	8
3.1 Basic equation	8
3.2 Advection	9
3.3 Vertical diffusion	9
3.4 Dry and wet deposition and chemical transformation	10
3.5 Emissions	11
3.6 Boundary values	12
4 RESULTS	12
4.1 January 1992	12
4.2 July 1992	13
5 FINAL REMARKS	14
6 REFERENCES	14
7 FIGURES	17

Preface and Acknowledgements

This note was prepared in time for the seventeenth session of the Steering Body of EMEP in order to give a status of the activity at MSC-W with regard to development and use of regional scale Eulerian models. The note presents a preliminary version of a regional scale multilayer model with 50km*50km horizontal resolution, together with the first results on sulphur transport and depositions in Europe based on this model. It must be noted that the results are preliminary and that it is too early to include estimates from the regional scale Eulerian model into the work on the protocols under the 1979 Geneva Convention on Long Range Transboundary Air Pollution.

The development of a regional scale Eulerian model is based on the meteorological data from a special version of the Numerical Weather Prediction model at The Norwegian Meteorological Institute. This version was set up by Professor T. Iversen and Senior Computer Consultant A. Foss during 1991. Without their efforts the present model development would have been considerably more difficult. The development has also strongly benefitted from the programming assistants of Programmer Analyst H. Styve.

The author also want to acknowledge valuable discussions and suggestions with the Professor's A. Eliassen and T. Iversen.

1 Introduction

At EMEP/MSC-W two-dimensional receptor oriented Lagrangian models have been used since the start of the programme. These models have quite successfully calculated annual concentrations and depositions of acidifying sulphur and nitrogen compounds, as well as long term concentrations of boundary layer ozone (Eliassen and Saltbones, 1983; Iversen, 1993; Sandnes, 1993; Simpson 1993). Calculations from these models have been employed quite extensively by subsidiary bodies under the 1979 Convention on Long Range Transboundary Air Pollution, supporting the discussions and negotiations for emission reduction protocols. The Lagrangian models are two-dimensional for the atmospheric boundary layer (ABL) with 150km*150km horizontal resolution. An important assumption in this model is that the emitted air pollutants are well mixed up to the top of the ABL. Such an assumption is justified by the coarse horizontal resolution employed in this model. Models with finer horizontal resolution will require several layers inside the ABL in order to describe the initial dispersion of the air pollutants properly. The multilayer approach is also needed in order to more thoroughly include the effects of windshear, vertical exchange between the ABL and the free troposphere and cloud chemistry. A finer horizontal resolution than 150km*150km is also desirable to better resolve small countries in Europe, and to better describe transport in mountainous areas.

Several multilayer Eulerian models have been developed with the purpose of analysing regional scale transport and deposition of air pollutants. The most well-known North American models are the RADM (Chang et al., 1987, McHenry et al., 1992), the ADOM (Venkatram et al., 1988) and the STEM-II model (Carmichael et al., 1986, 1991). A comparison and evaluation of the RADM and the ADOM are found in Dennis et al. (1990). A similar model, the EURAD model which is a modification of the RADM to fit European conditions, is presented in Hass et al. (1990). All these models are developed with a large degree of complexity in both the gas and liquid phase chemistry, and these models have so far only been used in episodic studies (days up to weeks) since their complexity has prohibited applications to longer term simulations. Berge (1993) has coupled a sulphur model including heterogeneous chemistry to a Numerical Weather Prediction model which may be run in real time simulations. A simpler Eulerian model for long term simulations is the LOTOS-model (Bultjes, 1992) which has been aiming at long term ozone simulations in Europe. At EMEP/MSC-W a hemispheric scale model (Iversen, 1989; Tarrason and Iversen, 1992) for long term simulations of sulphur transport between the continents has been developed.

As the requirements for more detailed information on the horizontal and vertical distribution of the air pollution are growing EMEP/MSC-W has started to develop a regional scale (50km*50km horizontal resolution) multilayer model. During this development we follow the earlier modelling approach within EMEP by making the model tools applicable to long term simulations. The first step in this development has been to establish a high quality meteorological data base. A special version of the Numerical Weather Prediction Model at the Norwegian Weather Service was therefore set up to provide complete meteorological data of 50 km horizontal resolution and a large number of layers in the vertical direction.

Our philosophy during the first phase of the development of the regional scale Eulerian model is to use a stepwise approach concentrating on simple chemical schemes, while transport formulation is more elaborate. It is then natural first to only consider sulphur components since its chemistry is relatively simple and emission data are available at EMEP/MSC-W for a large part of the northern hemisphere. During the course of the development we compare the Eulerian and Lagrangian models by letting the major differences be in the treatment of the transport terms and not in the chemistry. Consequently, we employ the linear transformation and deposition schemes for sulphur compounds which are found in the Lagrangian model (Sandnes, 1993). An important aspect of Eulerian models is the truncation errors related to the numerical solution of the advection equation. In Berge and Tarrason (1992) we reported on several numerical features of different numerical schemes for advection. The overall conclusion was that the Bott-scheme (Bott, 1989 a and b) was the best compromise between accuracy and computational costs among the schemes studied, and we therefore apply this scheme in the present development. The model also includes eddy transport in the vertical by calculating vertical eddy diffusivities in each model layer.

We would like to emphasize that the Eulerian model at EMEP/MSC-W is under continuous development and improvement and that only a preliminary model version and preliminary results are presented here. At the moment we are developing a generalized vertical coordinate system which will include the top of the ABL as a coordinate surface. The objective with such a coordinate system is to obtain a physically realistic description of the dispersion of the pollutants in the ABL and to use fewer layers in the vertical than in the present approach. A complete documentation of the regional scale Eulerian model will be given at a later stage.

We have performed the present model version for January 1992 and July 1992. In the discussions of the results we focus on a comparison with concentrations and deposition calculated with the Lagrangian approach. For the time being we are not able to include a model evaluation by comparison with measurements. This will indeed be given high priority in the future.

2 Meteorological data

A multilayer Eulerian air pollution model with 50km horizontal resolution requires a large amount of meteorological input data. In order to overcome this requirement a version of the Operational Numerical Weather Prediction (NWP) model of The Norwegian Meteorological Institute (DNMI) was set up in May 1991 (see Grønås et al. , 1987 and Nordeng, 1986, for a description of the NWP-models at DNMI). We will henceforth denote this particular version of the NWP-model for LAM50E (Limited Area Model, 50 km, Europe). The LAM50E is run in a six hourly intermittent data assimilation cycle with boundary values obtained from analysis made at the European Centre for Medium Range Weather Forecast. In the intermittent system observations from a period spanning the analysis time are used to correct a six hourly forecast made from the previous analysis. The

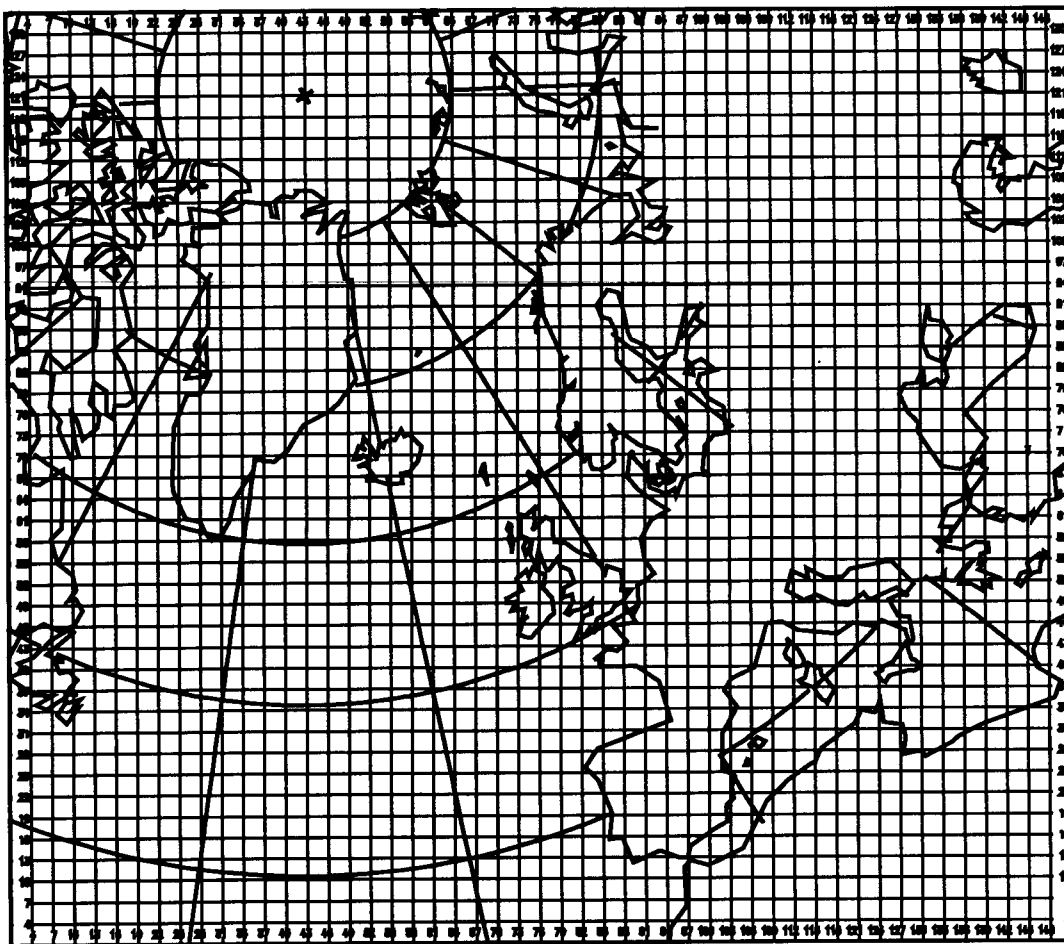


Fig.1 Calculation domain for the Eulerian model. One grid cell on the map corresponds to nine grid cells in the model.

analysis method is a modification of the successive correction method proposed by Bratseth (1986) and implemented for operational use at DNMI by Grønås and Midtbø (1987). A complete meteorological data set from a 6 hour forecast is then archived every six hour in 20 layers pluss the surface layer. The most important meteorological parameters in the archive are described in Table 1. The horizontal domain of the model was selected so that the 50km grid squares would coincide with the original EMEP-grid as presented in Sandnes (1993) (see Fig. 1). Moreover, the domain had to be extended far enough away from the area of main interest, namely Europe, in order to avoid that the meteorological calculations were dominated by the boundary conditions. This is particularly important in the westward direction since much of the “weather” originates from disturbances entering Europe from the west. Therefore the western boundary is quite far from the European continent. This is indeed also of importance for the chemical calculations since the western boundary will in the long term influence the calculations in Europe more than the other

boundaries. Nine of the layers in LAM50E are placed below 2 km (see Table 2) to obtain a high resolution of the boundary layer processes which are of special importance to the long range transport of air pollution. Also, the complete three dimensional cloud liquid water field is stored which opens for more detailed description of cloud chemical processes than has so far been possible within EMEP. The meteorological data applied to the air pollution modelling between the 6 hourly intervals are found by linear interpolation.

The output from the LAM50E to our data archive is about 36 MegaBytes (MB) per day. The use of this data base requires efficient program software before long term (months and years) run can be performed. Such software has to a large extent already been developed at DNMI for other purposes, and with the excellent guidance of the technical staff at DNMI the software has been modified to fit the development of the Eulerian model. With our present computing facilities it has then turned out to be convenient to run 1 month separately which makes the data management quite efficient and manageable (approximately 1 GigaByte (GB) of meteorological data is then included in one run). The computational efforts are considerable with a multilayer model that covers such a large domain as shown in Fig. 1. For the time being the model is run on a CRAY Y-MP4D/464. For future applications which may include gas and liquid phase chemistry even more powerful computational resources can be necessary. To be prepared for such developments a computer code of the Eulerian model applicable to massive parallel computing technics is under development. Results from this work will be reported in the future.

TABLE 1. The most important parameters included in the meteorological data archive.

Parameter	Output	Parameter	Output
U - x-componet of wind	3-D	P - rate of precipitation release	3-D
V - y-component of wind	3-D	p_S - surface pressure	surface
σ - vertical velocity in σ-coordinate	3-D	H_S - surface flux of sensible heat	surface
θ - potential tempera-tur	3-D	H_L - surface flux of latent heat	surface
q - specific humidity	3-D	τ - surface stress	surface
c_w - cloud liquid water	3-D	T_{2m} - temperature at 2m.	surface

TABLE 2. Height and thickness of the nine lowest layers in the Eulerian model.

Layer number	Approximate height	Approximate thickness
20	45 m	90 m
19	130 m	90 m
18	240 m	130 m
17	390 m	180 m
16	600 m	230 m
15	850 m	290 m
14	1150 m	340 m
13	1500 m	390 m
12	1900 m	440 m

3 Description of the Eulerian air pollution model.

In the following section we outline the main features of the present version of the Eulerian model.

3.1 Basic equation.

The equations are formulated in the same horizontal and vertical grid as the meteorological data. Hence a normalized vertical pressure coordinate (the sigma coordinate) together with a polar stereographic projection true at 60° N are employed. If we let ψ denote the mixing ratio (kg-sulphur/kg-air) of either SO₂ or particulate sulphate (SO₄) the continuity equation may be written (see for example Chang et al., 1987)

$$\begin{aligned} \frac{\partial}{\partial t}(\psi p^*) &= -m^2 \nabla_H \bullet (V_H \psi p^*) - \frac{\partial}{\partial \sigma}(\dot{\sigma} \psi p^*) \\ &+ \left[\frac{g}{p^*} \right]^2 \frac{\partial}{\partial \sigma} \left[\rho^2 K_Z \frac{\partial}{\partial \sigma}(\psi p^*) \right] + Q_S + Q_L \end{aligned} \quad (1)$$

The first two terms on the right hand side represent a flux divergence formulation of the advective transport. V_H and ∇_H are the horizontal wind vector and del operator respectively, and m is the map factor on a polar stereographic map projection. The vertical coordinate, σ , is defined as

$$\sigma = \frac{p - p_T}{p^*} \quad (2)$$

where $p^* = p_S - p_T$ and p , p_S and p_T are the pressure at level σ , the surface pressure and the pressure at the top of the model atmosphere respectively. p_T equals 100 hPa in the Eulerian model. The vertical velocity, $\dot{\sigma}$, equals $d\sigma/dt$. The third term in eq. (1) represents the vertical eddy diffusion where g , ρ and K_Z are the gravitational acceleration, air density and vertical eddy diffusion coefficient respectively. Horizontal eddy diffusion is not included in the model. Q_S and Q_L describe the other chemical and/or physical source or loss terms.

The time discretization of eq. (1) is performed with the fractional time step method (McRae et al., 1982). The different physical and chemical terms in the equation is then split into separate operators which are successively applied by intermediate time integrations. An example of the practical use of the fractional time step method to air pollution models is found in Berge (1993).

3.2 Advection

An important aspect of Eulerian models is the numerical errors caused by the numerical approximations to the advective part of eq. (1). Since advection in many cases is the largest source or loss term in eq. (1) the related errors must be considered carefully. In Berge and Tarrason (1992) several features of so-called flux schemes and pseudospectral schemes were discussed, and it was concluded that the Bott-scheme (Bott, 1989 a and b) could give a good compromise between accuracy and costs for a three-dimensional model. In the present model we utilize a fourth order version of the Bott-scheme in the horizontal and a second order version in the vertical where the model has variable grid distances.

Since the model experiments have been set up with a high vertical resolution close to the ground the Courant-Friedrich criteria ($V \cdot \Delta t / \Delta x < 1$) implies that a time-step of not more than about 5min can be applied to ensure numerical stability in the vertical direction. This is inconvenient since the time-step then is unnecessarily short for the physical accuracy of the model, and larger computational efforts are required than really necessary. This problem will indeed be improved since our intention is to employ fewer layers in the further development.

3.3 Vertical diffusion

The vertical sub-grid scale turbulent transport above the surface layer is described by application of diffusivity coefficients K_Z in eq. (1). The vertical diffusivities are not included in the data archive (see Table 1) and hence they have been derived from the basic meteorological parameters. We then follow the same procedure as utilized in the LAM50E which is described in Nordeng (1986). This formulation resembles Blackadar's (Blackadar, 1979) empirical formulae for K_Z where the local mixing length and the Richardson num-

ber are the most important quantities. An implicit method is applied to solve the vertical diffusion numerically.

In a similar fashion the drag coefficient in the surface layer is derived from the basic parameters in Table 1 using the same formulation as applied to LAM50E. The drag coefficient is used for the dry deposition calculations (see next section).

3.4 Dry- and wet deposition and chemical transformation.

The remaining source and loss terms treated here are dry- and wet deposition, chemical transformation and the release of emissions into a grid square. The dry deposition velocity for SO_2 at 1m, v_{1m} , is put equal to 0.8 cm s^{-1} over sea and it is somewhat lower over land depending on the latitude and the time of the year (see Sandnes, 1993, for further details). For particulate sulphate the deposition velocity at 1m equals 0.1 cm s^{-1} every where. In order to find the effective dry deposition velocity, v_{eff} , applicable to the concentrations at the lowest model level at approximately 45m (assumed to be the top of the surface layer) we employ the expression

$$v_{\text{eff}} = \frac{v_{1m}}{\left[1 + \frac{v_{1m}}{C_D |V_{45m}|} \right]} \quad (3)$$

where C_D is the drag coefficient and V_{45m} is the wind speed at the lowest model level.

The wet scavenging is calculated locally in each layer and summed in a column every time-step to obtain the deposition flux to the surface. The removal of sulphur in a layer is considered as the product of the precipitation rate, the concentration in air and a scavenging efficiency. The scavenging efficiency is given by the scavenging ratio which is taken from the Lagrangian model and set equal to $1.0 \cdot 10^6$ for particulate sulphate. For SO_2 it is expressed by

$$\Lambda = 3 \cdot 10^5 + 1 \cdot 10^5 \sin \left[2\pi \left(\frac{\tau - \tau_0}{\tau_a} \right) \right] \quad (4)$$

In this equation τ is the time of the year, τ_0 is 80 days and τ_a is one year. This formulation is included to account for the enhanced liquid phase formation and deposition of sulphate due to the higher concentrations of H_2O_2 in summertime than in wintertime.

The only chemical mechanism included in this model is the transformation of SO_2 to particulate sulphate. The oxidation rate, k_t , is given by

$$k_t = 3 \cdot 10^{-6} + 2 \cdot 10^{-6} \sin \left[2\pi \left(\frac{\tau - \tau_0}{\tau_a} \right) \right] \quad (5)$$

where the parameters in the sine-function are the same as for eq. (4). This model reaction parameterizes all possible oxidation pathways of SO₂ including gas phase and liquid phase reactions. In addition, 5% of the sulphur emissions are assumed to be in the form of particulate sulphate.

3.5 Emissions

At present no complete 50km emission data base exists for the EMEP-area. For the time being we have therefore utilized the 150km gridded emission data applied to the Lagrangian model. In the areas not covered by the EMEP data, emission values of 150km resolution from the Hemispheric scale model at EMEP/MSC-W (Tarrason and Iversen, 1992) are employed. To obtain 50km emissions we have made some simplifying assumptions described in the following. The horizontal distribution is found by simply dividing the 150km*150km values by 3*3. The seasonal variation in the source strengths follows a sine-function with an amplitude of 1.33 in January and 0.67 in July. In the vertical the EMEP data are separated into emissions below and above 100m for each grid square. We have used this information to make preliminary assumptions on a vertical distribution. We let the emissions below 100m be released in the lowest layer which extends up to about 90m (see Table 2). The emissions from high level sources will extend up to several hundred meters, but no data are available on the exact distributions. We have chosen to emit 50% of the high level emissions into the third level which extends from about 180m to 310m. The remaining 50% of the high level emissions are split in equal parts on the level above and below the third model level. This vertical distribution is consistent with what is used in other multilayer Eulerian models (Chang et al., 1987, Hass et al., 1990).

The preliminary calculations given in section 4 are for January and July 1992. The anthropogenic emissions taken from the Hemispheric model are however valid for 1985, while the data employed to the Eulerian model are mainly in the former Soviet Union for areas east of the standard EMEP-grid. We have scaled these emissions values according to the emission reduction of about 30% that has taken place in the period 1985 to 1992 in the former Soviet Union covered by the standard EMEP-grid (Sandnes, 1993).

We would like to stress that there is a strong need for more accurate emission data on 50km resolution before reliable calculations can be made with the present model. A quantification of the seasonal variation, and more detailed information on vertical emission distribution is also needed for the future model applications to sulphur transport.

An important feature of the Lagrangian model is that the emissions are assumed to be instantaneously well mixed up to the top of the mixing layer in a grid square of 150km*150km. Since in reality the mixing proceeds gradually, the pollutant will travel long distances (~ 100km) before it fills the mixed layer. During this process the ground

level concentrations are underestimated and consequently the dry deposition also will be underestimated. To adjust for this an additional local deposition is added to the Lagrangian model. In the multilayer approach we assume complete mixing of the emissions in each separate layer. The emissions closest to the surface are applied directly to the dry deposition process (eq. (3)) after being averaged over the lowest 90m thick layer. The situation is therefore very different from the one-layer approach and we have so far not included any additional local deposition in the multilayer model.

3.6 Boundary values.

At the lateral boundaries we have subjectively obtained values that correspond to monthly averages calculated with the Hemispheric scale model for 1988 (Tarrason, 1992).

4 Results

We have run the model for January and July 1992 in order to elucidate the model performance under different transport conditions. In the winter time stable conditions prevail over the continents in contrast to stronger vertical mixing and transport in the summer time. Also, the transformation rate and wet scavenging of sulphur are enhanced in the summer time (see eq. (4) and (5)). Average concentrations and accumulated dry and wet depositions are compared with results from the Lagrangian model. Unfortunately, we are not able to present comparisons with measurements at the present stage.

4.1 January 1992

We first present the concentration fields of SO_2 and particulate sulphate (Figs. 2 and 3). In the graphical display of the concentration fields they appear with zero values at the boundaries due to missing boundary values on the graphical files. This has of course not affected the model runs where non-zero boundary values have been employed. The concentrations are reduced to the surface (1m) values in the Lagrangian model, while they are referred to level 20 in the Eulerian model (approximately 45m). Consequently, the Eulerian values must be regarded somewhat lower at the surface than shown here. We observe that the concentration fields for both sulphur components coincide quite well in the two models, but some more details are indeed found in the Eulerian model due to the finer resolution. However, in areas far from the main sources the concentrations of both SO_2 and particulate sulphate are somewhat lower in the Eulerian approach than in the Lagrangian approach.

In Fig. 4 we see that the dry deposition patterns are very similar and resemble to a high degree the distribution of the emission sources. However, the peak values are considerably higher in the Lagrangian model than in the Eulerian model (not shown) due to the local deposition factor which is used in the Lagrangian approach. In northern latitudes the dry deposition is smaller over land than over sea in wintertime. This corresponds to the low deposition velocities applied to SO_2 over land in January.

The accumulated precipitation fields for January are shown in Fig. 5. Over land the precipitation field applied to the Lagrangian model is based on interpolation of measured data, while over sea the precipitation field is based on model calculations. The largest precipitation amounts are found over the relatively warm sea areas and at the western slopes of mountain barriers. The two fields correspond reasonable well over land which is encouraging in light of the present use of modelled precipitation instead of using measurements. The precipitation ceases near the boundaries of the Eulerian model due to the smoothing procedures applied to the LAM50E. We further present the accumulated wet deposition in Fig. 6. The most distinct feature is the considerably smaller wet deposition in the Eulerian model near the large source areas. This is may be not so surprising since the wet scavenging in the Eulerian model takes place locally in the layers where the precipitation is released, while the scavenging occurs in the atmospheric boundary layer in the Lagrangian model. In a stable winter atmosphere the transport of sulphur up to the clouds may be quite inefficient and hence relatively small amounts of sulphur are available for the wet scavenging. In more remote places more similar wet deposition patterns are found in the two models.

4.2 July 1992

In Fig. 7 and 8 we shown the SO₂ and sulphate concentrations in July as we did for January. Again we see a fairly good correspondance in the two patterns. However, the area with SO₂ values above 5 µg/m³ is considerably larger in the Eulerian model which may indicate too high surface concentrations in this model. This can partly be due to the differences in the treatment of the dry deposition. Furthermore, the surface concentrations are quite sensitive to the vertical distribution of the emissions and how well the vertical exchange mechanisms are parameterized. A similar pattern is reflected in the concentration fields for particulate sulphate (Fig. 8). In addition, we find somewhat higher sulphate values in more remote areas (Scandinavia) in the Eulerian model. In Fig. 9 we present SO₂ and sulphate fields for level 14 (approximately 1150m). It is worth to notice the considerably drop in specially the SO₂ concentrations near the large sources which may be due to a too weak vertical mixing.

The accumulated dry deposition patterns for July are shown in Fig. 10. As for January there are some few considerably higher peak values in the Lagrangian model in grid-squares with large emissions due to the local deposition factor (not shown). Except for this the patterns are quite similar.

The precipitation fields for July 1992 are compared in Fig. 11. For the summer month we observe relatively higher precipitation over land than over sea compared to January. This is what we would expect due to the convective precipitation over land in July. The two precipitation patterns agree fairly well over land, but somewhat larger areas with 100-200 mm are seen in the data based on measurements in Central Europe. On the other hand, the model produces higher values in some places in northern Scandinavia. The wet deposition (Fig. 12) in the Eulerian model is considerably smaller than in the Lagrangian model in parts of Central Europe. It is not likely that the differences can be attributed to the lower precipitation amount in the modelled data only. This is in particular obvious near the large source areas in Great Britian, where the precipitation amounts are quite similar in

the two models. On the other hand we see larger wet deposition in more remote areas such as northern Scandinavia using the multilayer approach.

5 Final remarks

In this note we have shown some preliminary results for January and July 1992 from a first version of the regional scale Eulerian model at MSC-W. Since no comparison with measurements yet has been made we are careful in drawing any firm conclusions from this work. However, we find the results encouraging and an important finding is that the calculated sulphur concentrations and depositions correspond quite well for the Eulerian and Lagrangian model. The largest discrepancies between the two models are in the wet deposition which is higher near the source areas in the Lagrangian model both for January and July. In parts of Scandinavia the Eulerian model gives the highest wet deposition in July. The near surface concentrations in July are considerably higher near the large emission areas in the Eulerian model than in the Lagrangian model. This is probably related to differences in the treatment of the dry deposition and the vertical mixing.

At present the further development of the Eulerian model is focused on introducing a general vertical coordinate system which considers the mixing height as one coordinate surface. We will then be able to address the vertical mixing problem in a more satisfactory way than we have been able to do so far.

There is also a clear need for improvement of the treatment of the dry and wet scavenging processes. Our future aims are to include parameterizations of in-cloud chemical processes. This may require coupling to photochemistry, and it is therefore a considerably modelling challenge. Similarly, our intention is to include more detailed information on the surface properties within each individual grid square in order to improve the estimates of the dry deposition fluxes.

Finally, we would like to stress that a weak point is the emission data. There are however, reasons to believe that more reliable 50km*50km emission data bases will become available within EMEP in the future through the on-going activities under the UN-ECE Task Force on Emissions and its collaboration with the EEC- emission programme CORINAIR.

6 References.

- Berge, E. 1993. Coupling of wet scavenging of sulphur to clouds in a numerical weather prediction model. *Tellus* 45B, 1-22.
- Berge, E. and Tarrason, L. 1992. An evaluation of eulerian advection methods for the modelling of long range transport of air pollution. EMEP/MSC-W, Note 2/92. The Norwegian Meteorological Institute, Oslo, Norway.

- Blackadar, A. K. 1979. High resolution models of the planetary boundary layer. *Advances in Environment and Scientific Engineering*, 1. Gordon and Branch, 276 pp.
- Bott, A. 1989a. A positive definite advection scheme obtained by non-linear renormalization of the advective fluxes. *Mon. Wea. Rev.* 117, 1006-1015.
- Bott, A. 1989b. Reply. *Mon. Wea. Rev.* 117, 2633-2636.
- Bratseth, A. M. 1986. Statistical interpolation by means of successive corrections. *Tellus* 38A, 438-447.
- Builtjes, P. J. H. 1992. The LOTOS - Long term ozone simulation-project. Summary report. TNO-report IMW-R 92/240, TNO Environmental and Energy Research, Delft, The Netherlands.
- Carmichael, G. R., Peters, L. K. and Kitada, T. 1986. A second generation model for regional-scale transport/chemistry/deposition. *Atmos. Environ.* 20, 173-188.
- Carmichael, G. R., Peters, L. K. and Saylor, R. D. 1991. The STEM-II regional acid deposition and photochemical oxidant model-1. An overview of model development and applications. *Atmos. Environ.* 25A, 2077-2090.
- Chang, J. S., Brost, R. A., Isaksen, I. S. A., Madronich, P., Stockwell, W. R. and Walcek, C. J. 1987. A three-dimensional Eulerian acid deposition model: Physical concepts and formulation. *J. Geophys. Res.* 92, 14681-14700.
- Dennis, R. L., Barchet, W. R., Clark, T. L., Seilkop, S. K. and Roth, P. M. 1990. Evaluation of regional acidic deposition models (part 1), NAPAP SOS/T Report 5. In National Acid Precipitation Assessment Program, Acidic Deposition: State of Science and Technology, Vol. 1. 722 Jackson Place, NW, Washington, DC.
- Eliassen, A. and Saltbones, J. 1983. Modelling of long-range transport of sulphur over Europe.: A two year model run and some model experiments. *Atmos. Environ.* 22, 1457-1473.
- Grønås, S., Foss, A. and Lystad, M. 1987. Numerical simulations of polar lows in the Norwegian Sea. *Tellus* 39A, 334-352.
- Grønås, S. and Midtbø, K. H. 1987. Operational multivariate analysis by successive corrections. *J. Meteorol. Soc. Jpn.*, WMO/IUGG/NWP, Symp., Special issue, 61-74.
- Hass, H., Jakobs, H. J., Memmesheimer, M., Ebel, A. and Chang, J. S. 1990. Simulation of a wet deposition case in Europe using the European Acid Deposition Model (EURAD). 18th ITM on Air Pollution Modelling and its Applications. Vol. 1, 153-160.
- Iversen, T. 1989. Numerical modelling of the long range atmospheric transport of sulphur dioxide and particulate sulphate to the arctic. *Atmos. Environ.* 23, 2571-2595.

- Iversen, T. 1993. Modelled and measured transboundary acidifying pollution in Europe-Verification and trends. *Atmos. Environ.* 27A, 889-920.
- McHenry, J. N., Binkowski, F. S., Dennis, R. L., Chang, J. S. and Hopkins D. 1992. The tagged species engineering model (TSEM). *Atmos. Environ.* 26A, 1427-1443.
- McRae, G. J., Goodin, W. R. and Seinfeld, J. H. 1982. Numerical solution of the atmospheric diffusion equation for chemically reacting flows. *J. Comp. Phys.* 45, 1-42.
- Nordeng, T. 1986. Parameterization of physical processes in a three-dimensional numerical weather prediction model. Technical Report no. 65, The Norwegian Meteorological Institute, Oslo, Norway.
- Sandnes, H. 1993. Calculated budgets for airborne acidifying components in Europe, 1985,1987,1988,1989,1990,1991 and 1992. EMEP/MSC-W, Report 1/93. The Norwegian Meteorological Institute, Oslo, Norway.
- Simpson, D. 1993. Photochemical model calculations over Europe for two extended summer periods: 1985 and 1989. Model results and comparison with observations. *Atmos. Environ.* 27A, 921-943.
- Tarrason, L. and Iversen T. 1992. The influence of north American anthropogenic sulphur emissions over western Europe. *Tellus* 44B, 114-132.
- Tarrason, L. Contributions to sulphur background deposition over Europe: Results for 1988. EMEP/MSC-W, Note 5/92. The Norwegian Meteorological Institute, Oslo, Norway.
- Venkatram, A. Karamchandani, P. K. and Misra, P. K. 1988. Testing a comprehensive acid deposition model. *Atmos. Environ.* 22, 737-747.

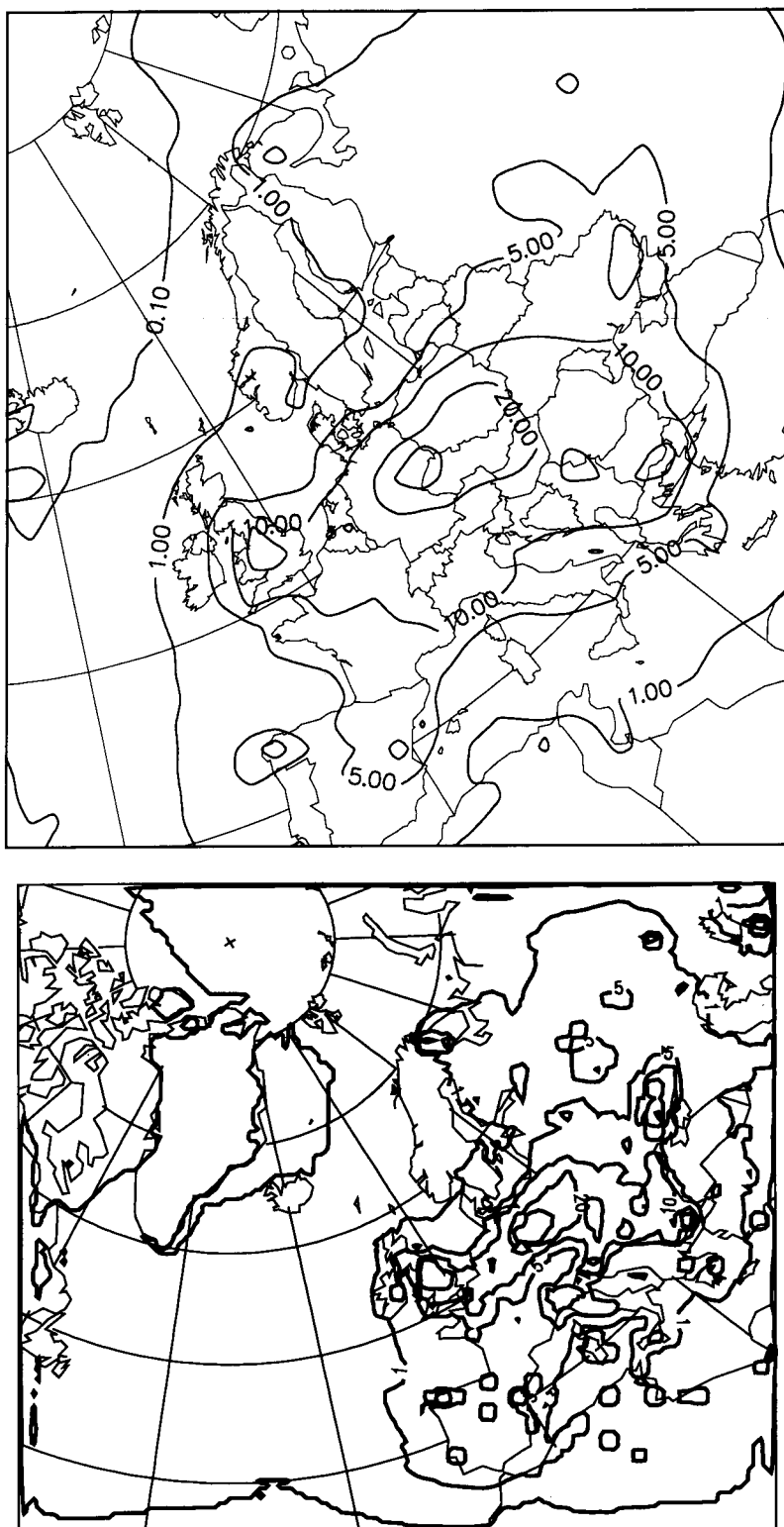


Fig. 2. SO₂ concentration in air at the surface for January 1992 calculated with the Lagrangian model (above) and the Eulerian model (below). Isolines are for 0.1, 1.0, 5.0, 10.0, 20.0 and 40.0 μg(S)/m³.

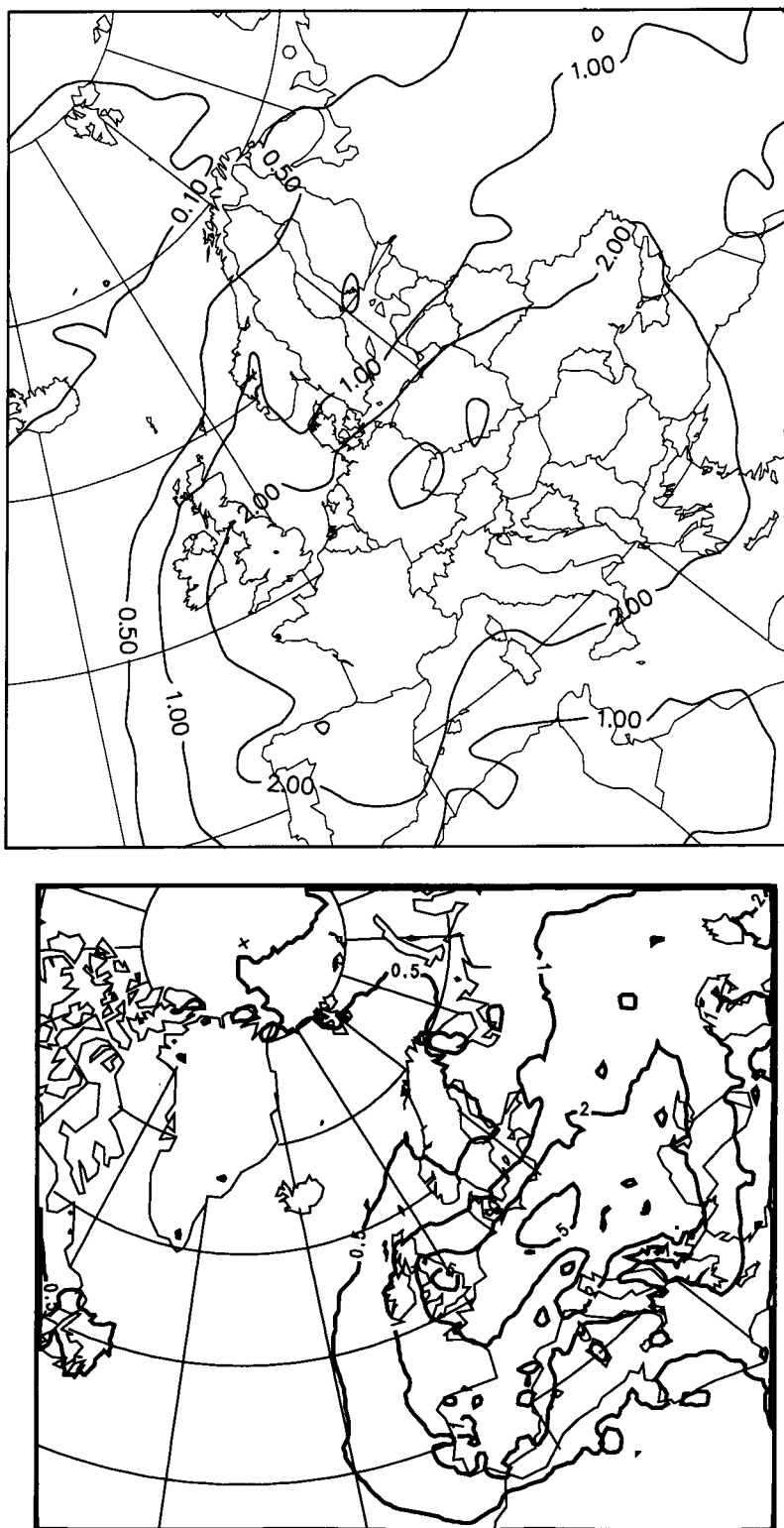


Fig. 3. Concentration of particulate sulphate in air at the surface for January 1992 calculated with the Lagrangian model (above) and the Eulerian model (below). Isolines are for 0.1, 0.5, 1.0, 2.0 and 5.0 $\mu\text{g}(\text{S})/\text{m}^3$.

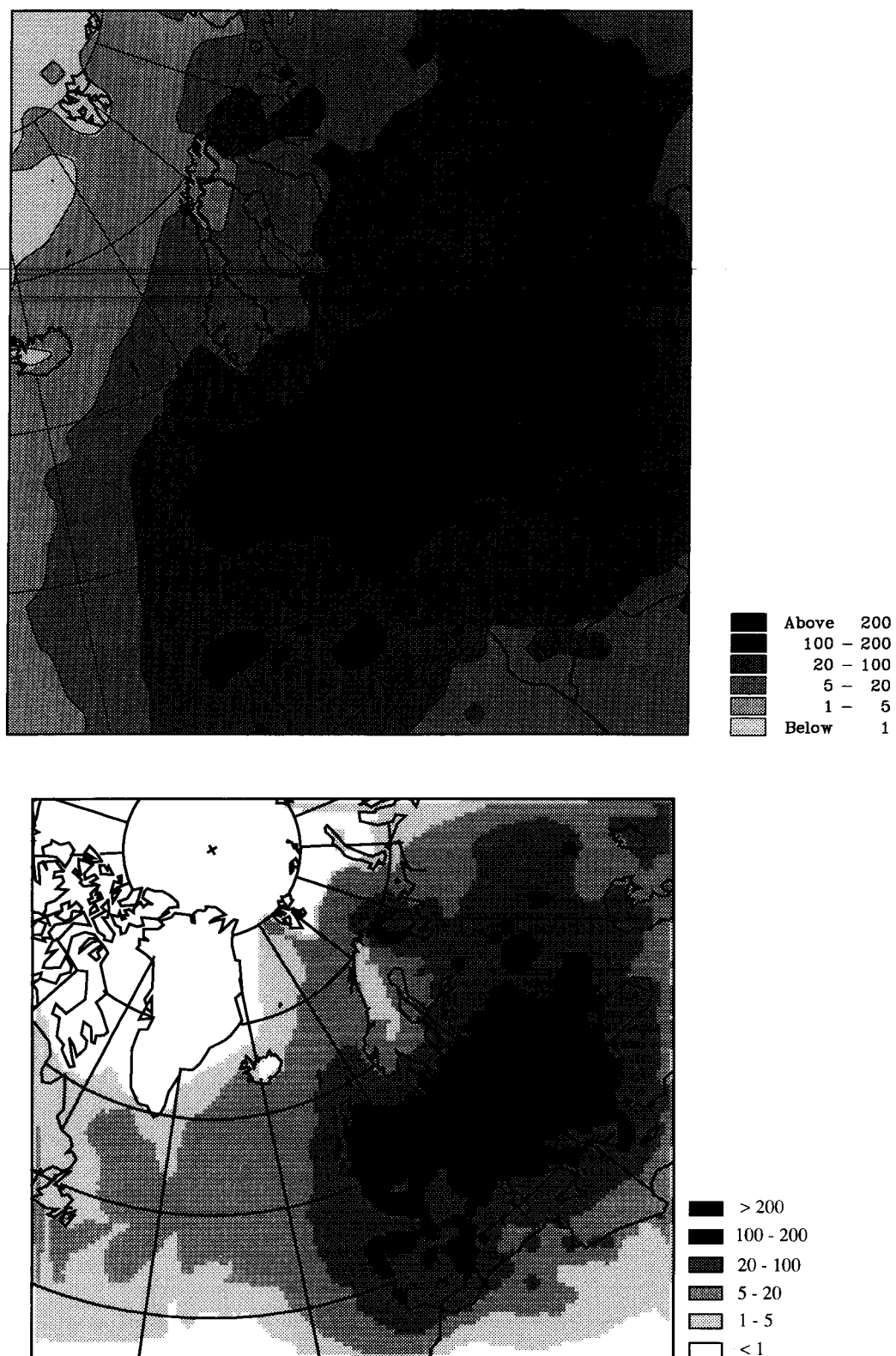


Fig. 4. Accumulated dry deposition of sulphur (mg(S)/m^2) for January 1992 calculated with the Lagrangian model (above) and the Eulerian model (below).

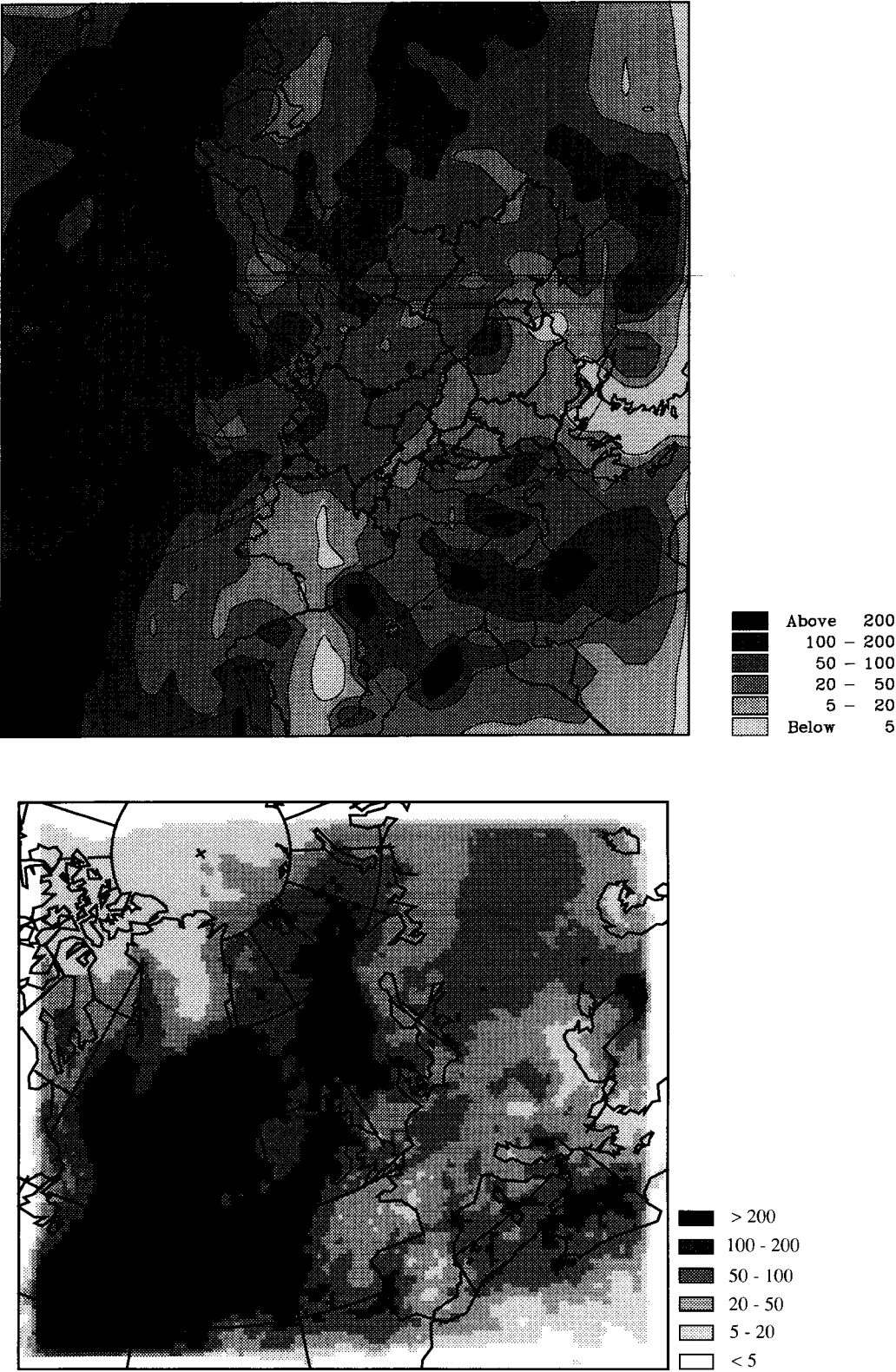


Fig. 5. Accumulated precipitation (mm) for January 1992 applied to the Lagrangian model (above) and the Eulerian model (below).

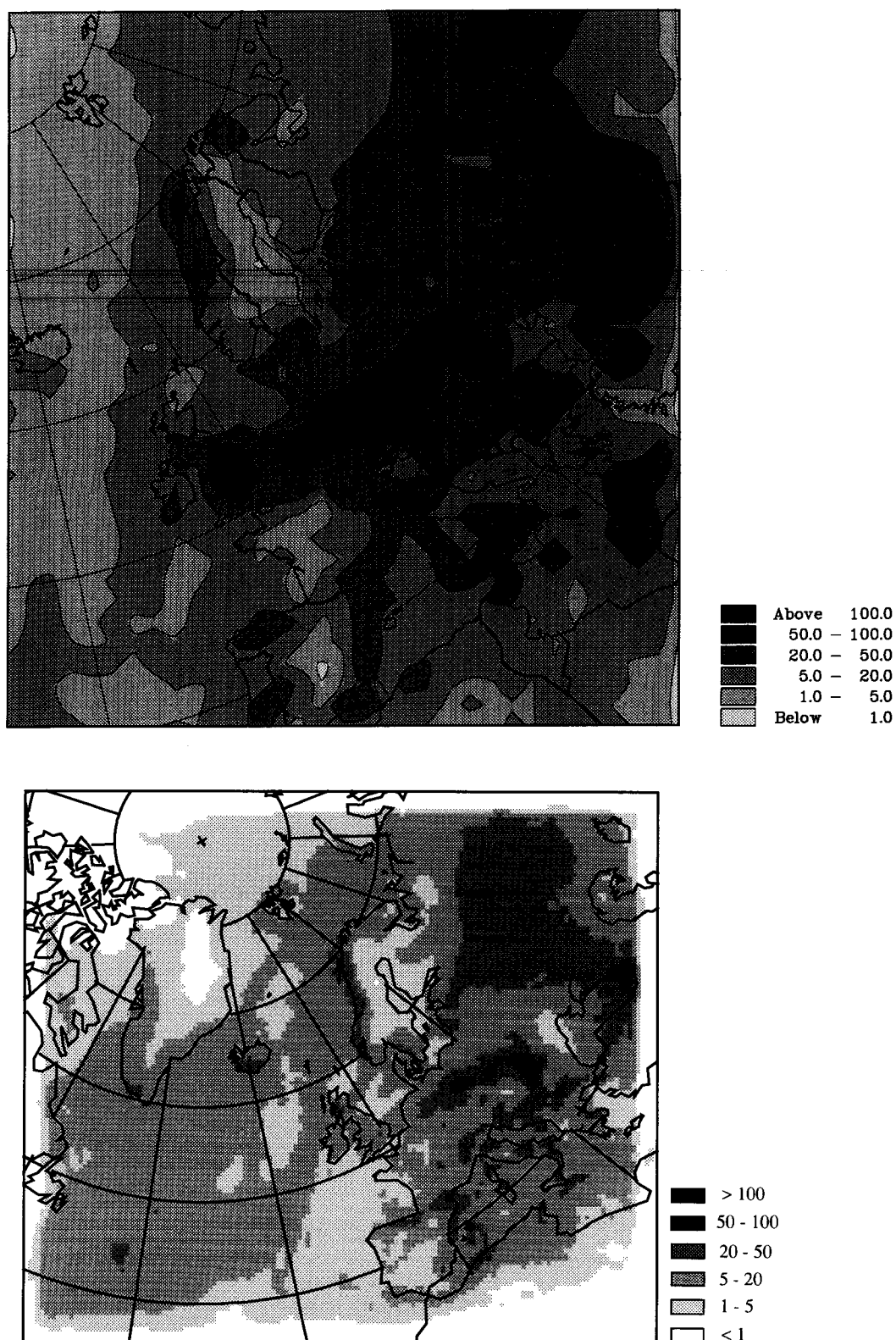


Fig. 6. Accumulated wet deposition of sulphur ($\text{mg}(\text{S})/\text{m}^2$) for January 1992 calculated with the Lagrangian model (above) and the Eulerian model (below).

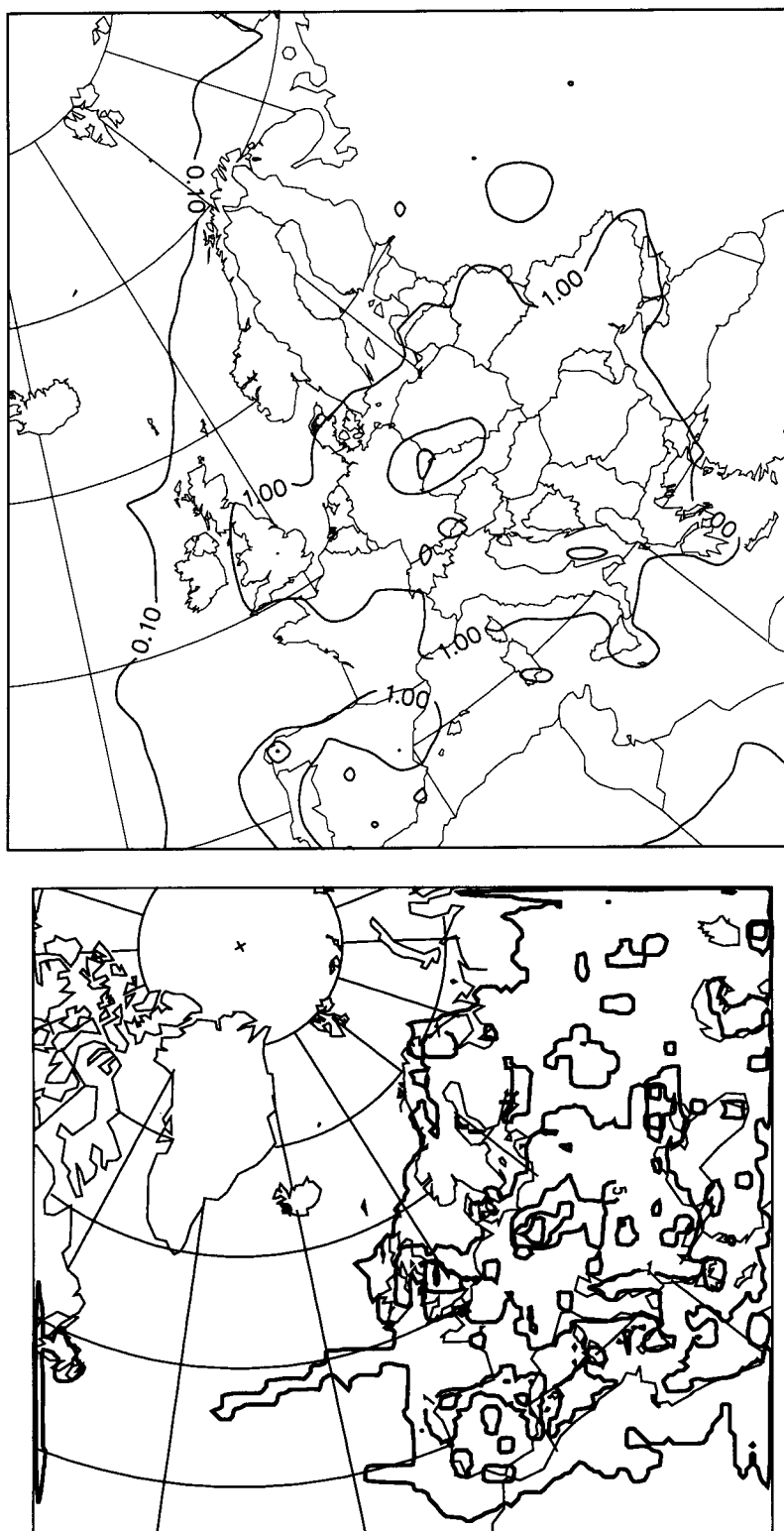


Fig. 7. SO₂ concentration in air at the surface for July 1992 calculated with the Lagrangian model (above) and the Eulerian model (below). Isolines are for 0.1, 1.0, 5.0, 10.0, 20.0 and 40.0 $\mu\text{g}(\text{S})/\text{m}^3$.

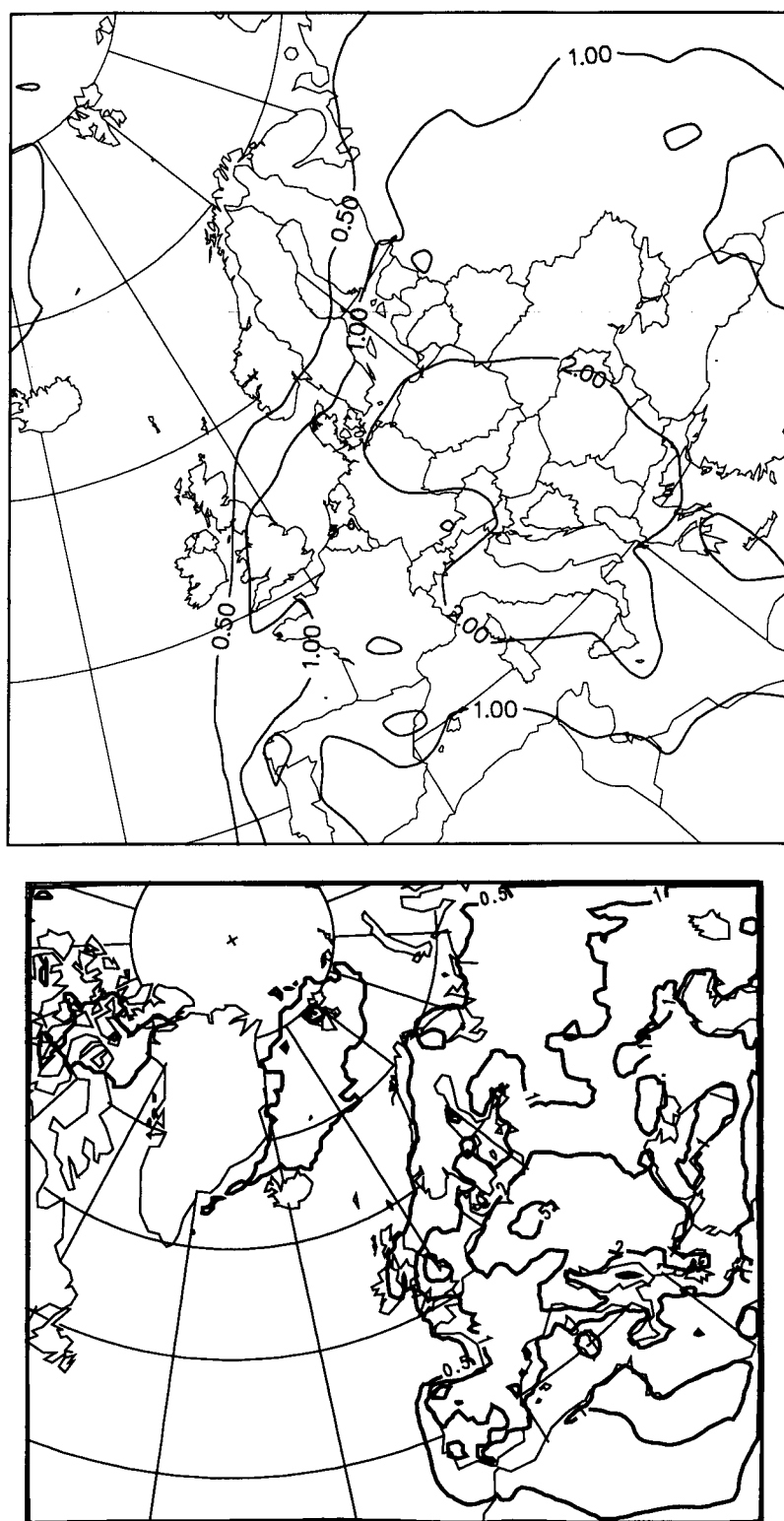


Fig. 8. Concentration of particulate sulphate in air at the surface for July 1992 calculated with the Lagrangian model (above) and the Eulerian model (below). Isolines are for 0.1, 0.5, 1.0, 2.0 and 5.0 $\mu\text{g}(\text{S})/\text{m}^3$.

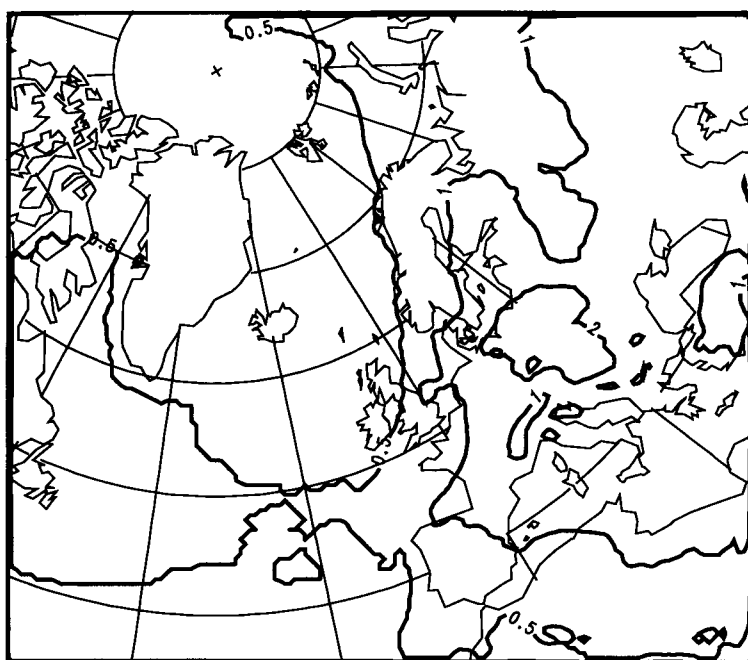
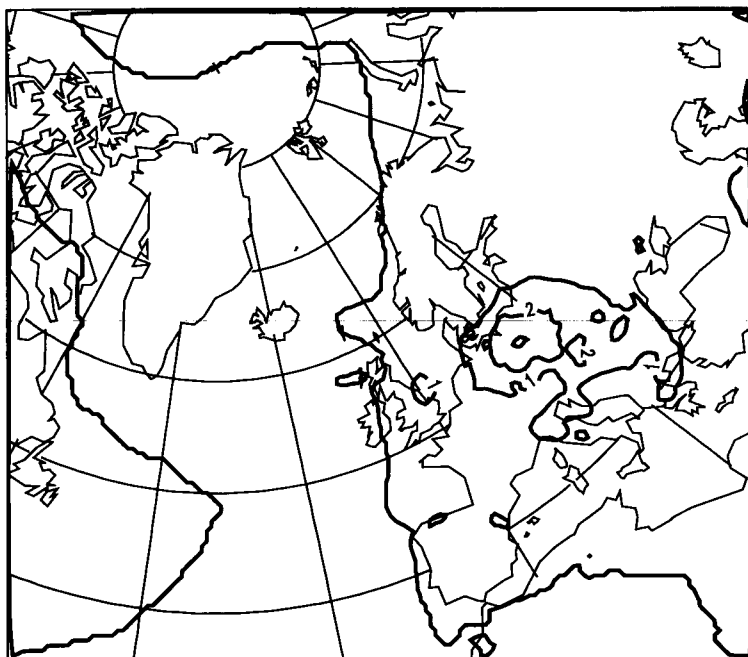


Fig. 9. Concentrations in air of SO_2 (above) and particulate sulphate (below) in level 14 (approximately 1150 m) in July. The isolines are 0.1, 1.0, 2.0 and 4.0 $\mu\text{g(S)}/\text{m}^3$ for SO_2 and 0.1, 0.5, 2.0 and 5.0 $\mu\text{g(S)}/\text{m}^3$ for particulate sulphate.

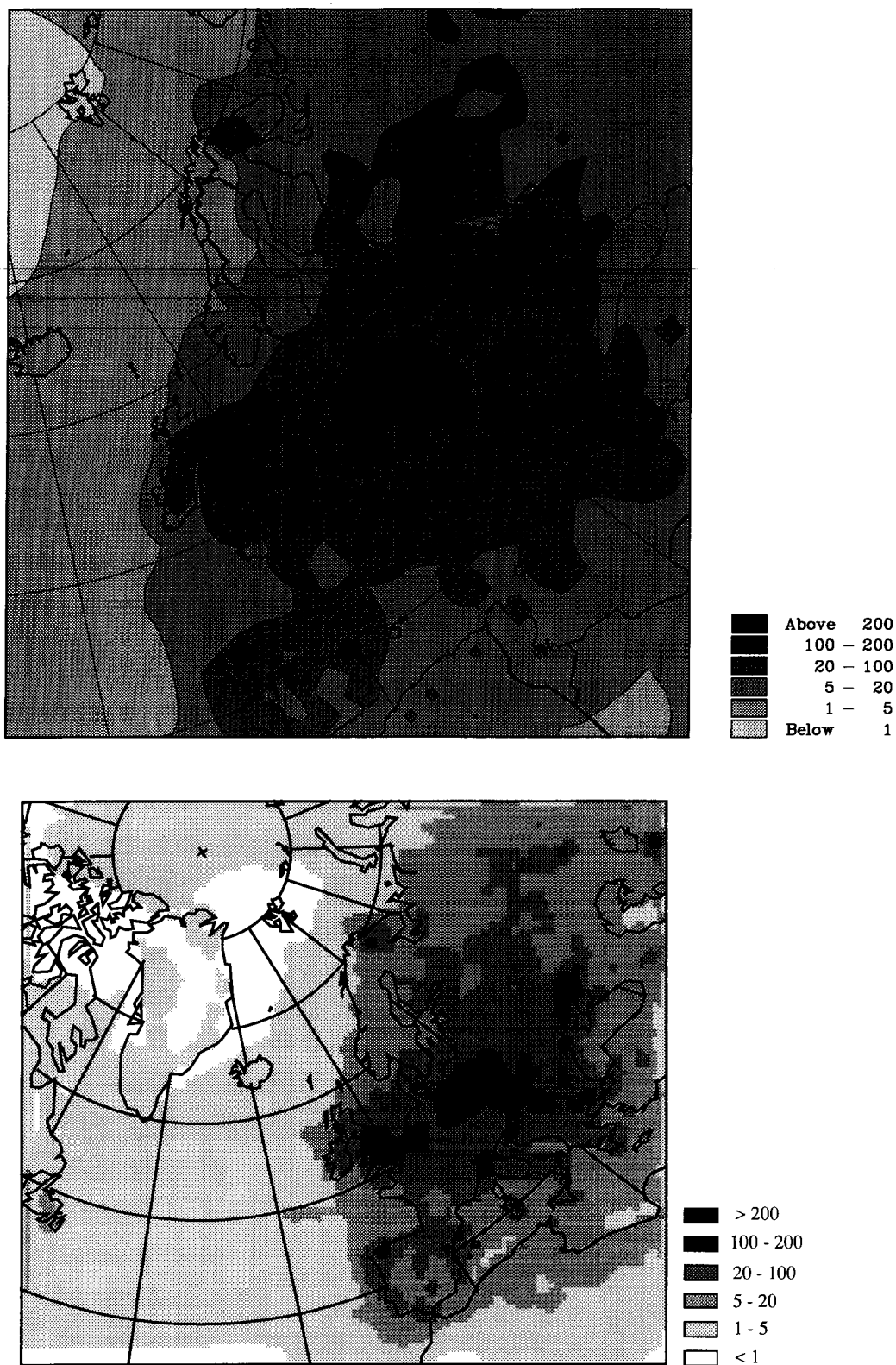


Fig. 10. Accumulated dry deposition of sulphur (mg(S)/m^2) for July 1992 calculated with the Lagrangian model (above) and the Eulerian model (below).

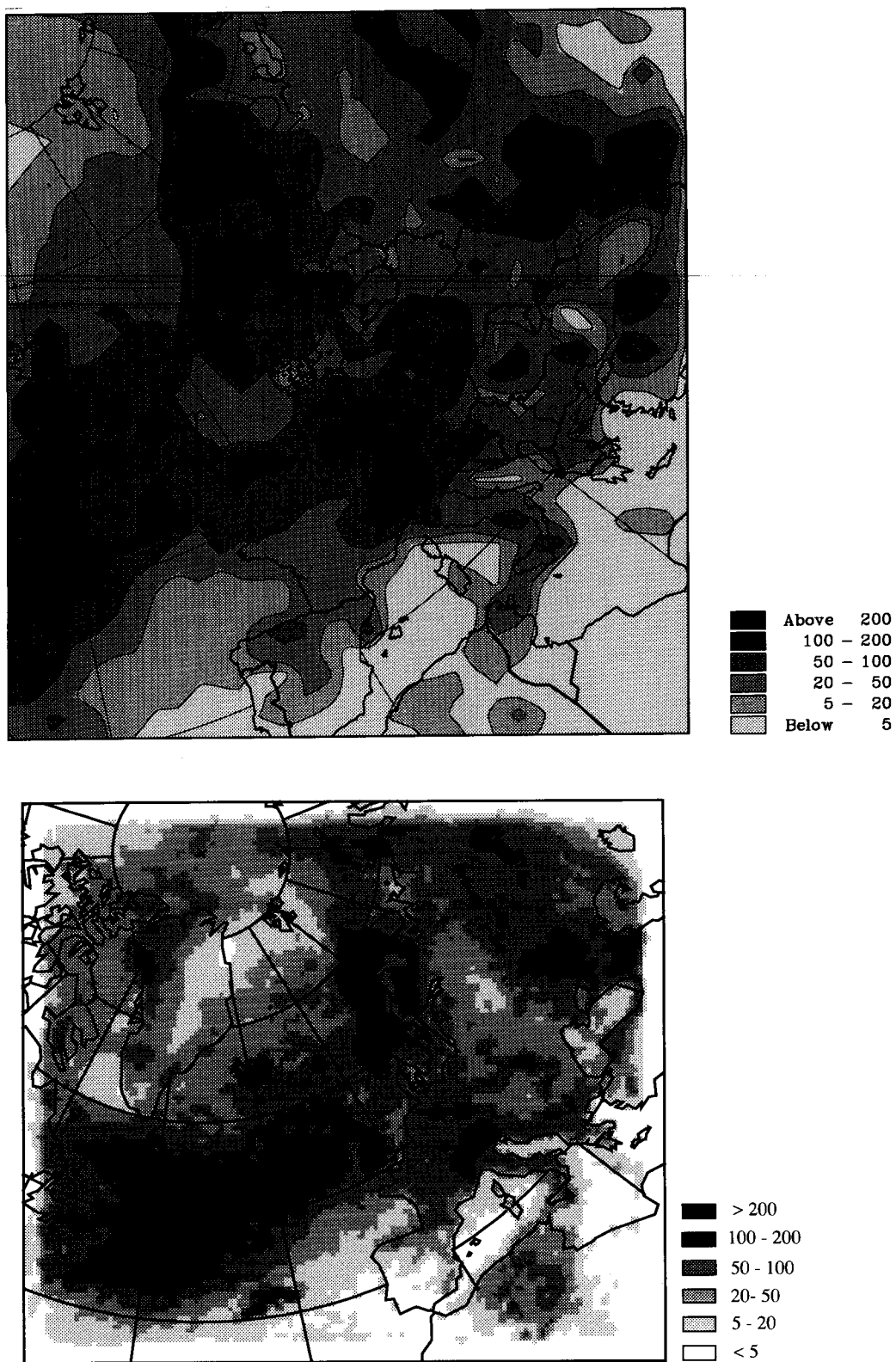


Fig. 11. Accumulated precipitation (mm) for July 1992 applied to the Lagrangian model (above) and the Eulerian model (below).

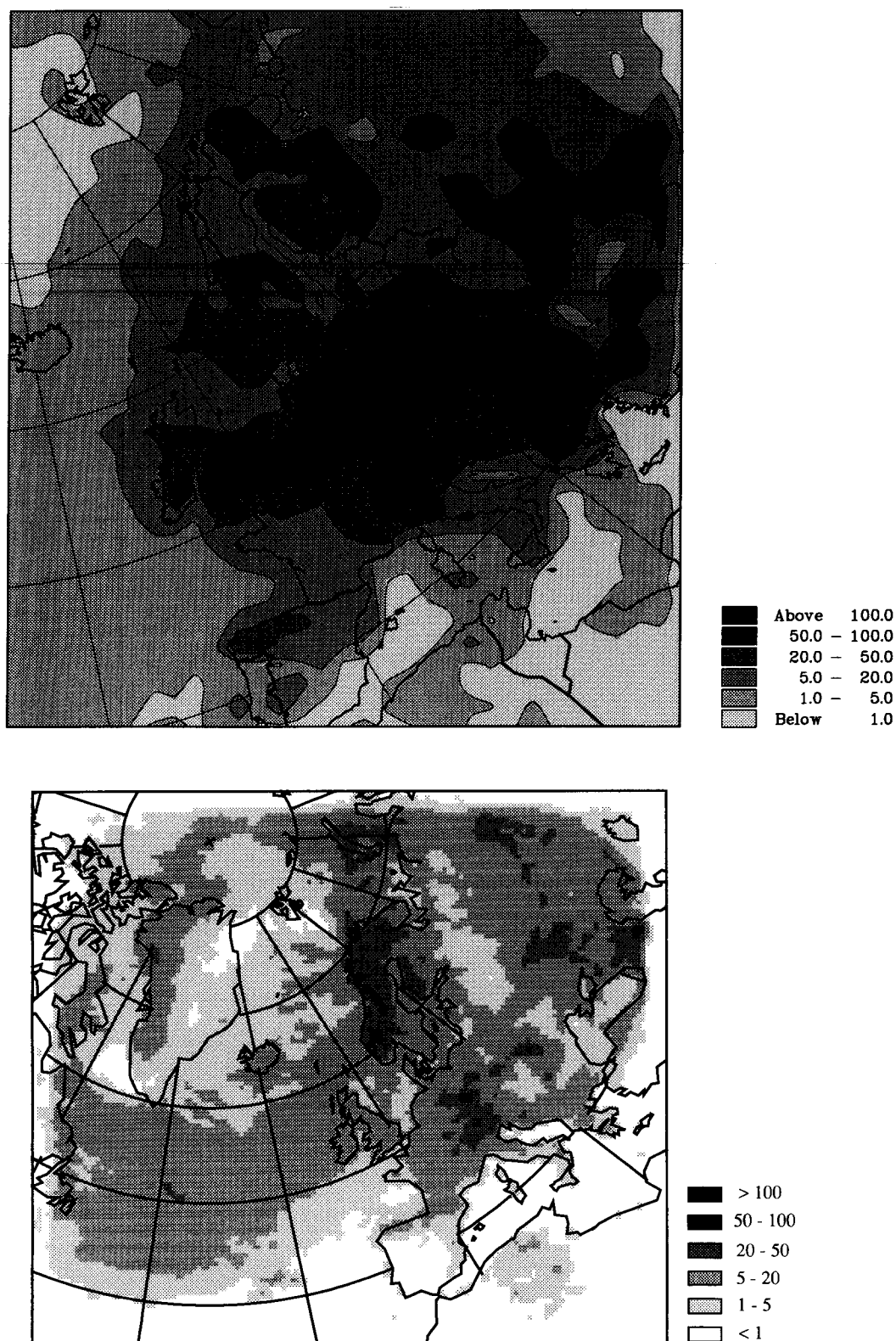


Fig. 12. Accumulated wet deposition of sulphur (mg(S)/m^2) for July 1992 calculated with the Lagrangian model (above) and the Eulerian model (below).

the 1990s, the number of people in the world who are undernourished has increased from 600 million to 800 million (FAO 1996).

There is a growing awareness of the need to address the problem of undernourishment. The United Nations World Food Conference in 1996, for example, set a target of halving the number of undernourished people in the world by the year 2015. The World Bank has also set a target of halving the number of undernourished people in the world by the year 2020 (World Bank 1996).

There are a number of reasons why the number of undernourished people in the world has increased. One of the main reasons is the rapid population growth in the developing world. The population of the world is expected to reach 8 billion by the year 2025, with the majority of the increase occurring in the developing world (United Nations 1996).

Another reason for the increase in undernourishment is the rapid growth in the number of people living in poverty. The number of people living on less than \$1 a day has increased from 1.2 billion in 1981 to 2.1 billion in 1996 (World Bank 1996). This increase in poverty has led to a decrease in the amount of food that people can afford to buy.

A third reason for the increase in undernourishment is the rapid growth in the number of people living in urban areas. The number of people living in urban areas has increased from 1 billion in 1981 to 2.5 billion in 1996 (United Nations 1996). This increase in urbanization has led to a decrease in the amount of food that people can afford to buy.

There are a number of ways in which the problem of undernourishment can be addressed. One way is to increase the production of food. This can be done by increasing the amount of land that is used for agriculture, by increasing the amount of fertilizer that is used, and by increasing the amount of water that is used for irrigation.

Another way to address the problem of undernourishment is to increase the income of people living in poverty. This can be done by providing them with access to credit, by providing them with training in agriculture, and by providing them with access to markets.

A third way to address the problem of undernourishment is to increase the amount of food that is available to people living in urban areas. This can be done by providing them with access to public markets, by providing them with access to community gardens, and by providing them with access to food banks.

There are a number of challenges that must be overcome in order to address the problem of undernourishment. One of the main challenges is the need to increase the production of food. This requires a significant increase in the amount of land that is used for agriculture, which is a challenge in many developing countries.

Another challenge is the need to increase the income of people living in poverty. This requires a significant increase in the amount of credit that is available to people living in poverty, which is a challenge in many developing countries.